QUANTUM SIMULATIONS OF QCD WITHIN A PARTICLE-BASED ENCODING*

J.J. Gálvez-Viruet

Departamento de Física Teórica & IPARCOS
Universidad Complutense de Madrid, 28040 Madrid, Spain

Nicolás Martínez de Arenaza

Instituto de Física Teórica UAM-CSIC, 28049 Madrid, Spain

Received 6 April 2026, accepted 29 April 2026, published online 10 July 2026

We describe an algorithm to calculate fragmentation functions from first principles by using quantum computers. The algorithm is grounded in an encoding paradigm in which particles and their internal degrees of freedom are the central objects, and its main step consists of evolving an initial parton using the Light-Front Hamiltonian.

DOI:10.5506/APhysPolBSupp.19.4-A8

1. Introduction

High-energy scattering involving hadrons is described in terms of a small number of constituents called partons which, however, do not appear in the final states. Instead, after the perturbative interaction, the partons devolve non-perturbatively into colorless objects. Factorization theorems allow for a separate description of these two regimes, making it possible to describe the non-perturbative part in terms of universal kernels known as *fragmentation functions*. The definition of a bare fragmentation function describing how an initial charm quark with spin j evolves into a final J/Ψ meson carrying a momentum fraction z is [1] as follows:

$$D_j^{J/\Psi}(z) \equiv \frac{\mathrm{Tr}_m\,\mathrm{Tr}_c}{3\,N_{c,j}} \sum_X \langle p,j,c|J/\Psi(z,m),X\rangle_{\mathrm{out}}\langle J/\Psi(z,m),X|_{\mathrm{out}}|p,j,c\rangle\,, \tag{1}$$

where Tr_m is a trace over meson polarizations and Tr_c over quark colors. If the meson factorizes from the remaining fragmentation products,

* Presented at the Excited QCD 2026 Workshop, Granada, Spain, 8–14 January, 2026.

$|h_s, X\rangle_{\text{out}} = |h_s\rangle_{\text{out}}|X\rangle_{\text{out}}$. By $\sum_X |X\rangle_{\text{out}}\langle X|_{\text{out}} = \mathcal{I}$, we have

$$D_j^{J/\Psi}(z) \equiv \frac{\text{Tr}_m \,\text{Tr}_c}{3\, N_{c,j}} |\langle J/\Psi(z,m)|_{\text{out}}|p,j,c\rangle|^2 \,. \tag{2}$$

The standard procedure to address non-perturbative QCD is to discretize space and sample gauge configurations. The time-direction is usually transformed into a space-like direction by means of a Wick rotation, arriving at a Euclidean action. This prevents access to real-time phenomenology and fragmentation functions.

One possible way out is to simulate the process in quantum computers. Other works have considered fragmentation functions within the NJL model [2]. Here, we explain how to calculate them starting from the Light-Front Hamiltonian of QCD.

2. Light-Front Hamiltonian

The dynamics of highly relativistic partons are most conveniently described in light-front coordinates $(x^+, x^-, x^\perp)$. The evolution of the initial parton into the space-time point in which the meson is measured is, in general, implemented through the light-cone generators P^- and $P^\perp$. The transverse momentum is, however, taken to be zero here, so that $\Delta x^\perp = 0$. The bare fragmentation function then reads

$$D_j^{J/\Psi}(z) = \frac{1}{3}\sum_m \frac{1}{N_c}\sum_c \left|\left\langle \psi_{J/\Psi}(z;m)\right| \mathrm{e}^{-iP^- x^+} |p,j,c\rangle\right|^2 . \tag{3}$$

In order to compile the exponential $\mathrm{e}^{-iP^- x^+}$, the Light-Front Hamiltonian P^- [3] is written in terms of creation and annihilation operators. Each operator-product is then an interaction vertex and has a diagramatic representation, see Fig. 1. An example of such interactions is the quark–gluon

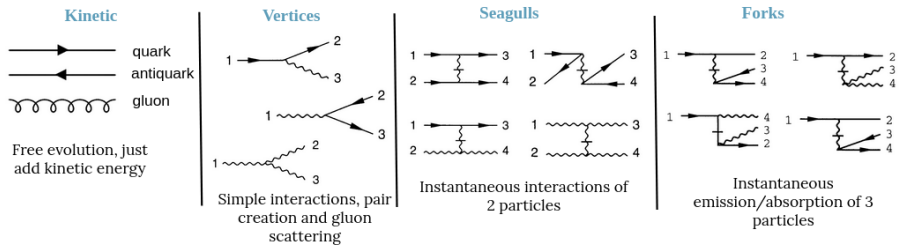

Fig. 1. Examples of the Light-Front Hamiltonian P^- interaction vertices; see [3] or [9] for a complete list. Time flows to the left. Straight lines represent fermions, wavy lines gluons, and cut lines denote insertions of the light-front potential.

splitting kernel $V_1 = \int V_1(1;2,3)\,(b_1^\dagger b_2 a_3 + \text{h.c.})$, where subindices 3 (1, 2) index gluon (quark) quantum numbers. The three-momentum is conserved at each vertex and all particles are on shell. $V_1(1;2,3)$ is a function of quantum numbers which can be found in [3] or Appendix A of [9].

3. Encoding and time evolution

Quantum hardware is able to execute only a small universal set of quantum gates. Therefore, arbitrary unitary operators, such as $\exp(-iP^-\Delta x^+)$, must be compiled. An example of a universal set consists of single-qubit rotations $\mathtt{R}_i(\theta)$, Pauli gates $\mathtt{X}, \mathtt{Y}, \mathtt{Z}$, and 2-qubit controlled-$\mathtt{X}$ (`CNOT`) gates.

The encoding used here [4] is based on transformations between particle states, implemented through a representation of creation and annihilation operators. The first step is to assign qubits to *particle registers*

$$\left|\widetilde{\Omega}\right\rangle_g = |0\rangle_\exists \otimes \left(|0\rangle^{\otimes\lceil\log\left(N_c^2-1\right)\rceil}\right) \otimes \left(|0\rangle^{\otimes\lceil\log N_s\rceil}\right) \otimes \left(|0\rangle^{\otimes\lceil\log N_p\rceil}\right), \tag{4}$$

where $|0\rangle_\exists$ is an auxiliary qubit, N_c, N_s, and N_p are the numbers of color, spin, and momentum degrees of freedom of gluons (fermion registers are analogous). Creation and annihilation operators are then written in terms of elementary transformations on these registers

$$a_1^{(n)\dagger} = \sum_{j=1}^{n} \mathcal{S}_j \cdot P_0^{(n-j)} \otimes \left(C_{10} \otimes s_1^\dagger\right)_j \otimes P_{j-1}^{(j-1)}, \tag{5}$$

where the symbol $\cdot$ separates independent sets of operations. The ones to the right of $\cdot$ apply the *set* operator $s_1^\dagger$ to register j, initializing it to configuration 1, while the single-qubit transformation C_{10} initializes a *presence* qubit. These operations are conditioned by the projectors P, which must evaluate to one for the creation operator to act, *i.e.* the previous $j-1$ registers must be occupied and the following $n-j$ registers must be empty. Finally, $\mathcal{S}_j$ symmetrizes the state of register j with those of the remaining registers.

The number of terms in Eq. (5) depends on the number of particles. In this work, we have considered memories with the capacity for up to 2 quarks, 1 gluon, and 1 antiquark. Operator-products such as that of V_1 now read

$$\begin{aligned} b_1^\dagger b_2 a_3 \;=\; & P_0^{(1_f)} \otimes \left(C_{11} \otimes s_1^\dagger s_2\right)_{1_f} \bar{\otimes}\, (C_{01} \otimes s_3)_{1_g} \\ & + \mathcal{A}_{2_f} \cdot \left(C_{11} \otimes s_1^\dagger s_2\right)_{2_f} \otimes P_1^{(1_f)} \bar{\otimes}\, (C_{01} \otimes s_3)_{1_g} \cdot \mathcal{A}_{2_f}, \end{aligned} \tag{6}$$

where $\bar{\otimes}$ separates transformations between registers of different particle types. These operators can then be exponentiated and compiled, see [4].

Finally, note that, as different terms in P^- do not commute, their separate exponentiation introduces errors. These can be systematically reduced by using the Trotter formula

$$\mathrm{e}^{-i\Delta t\,(A+B)} = \left(\mathrm{e}^{-iA\Delta t/n}\,\mathrm{e}^{-iB\Delta t/n}\right)^n + \mathcal{O}\left((\Delta t/n)^2\right) . \tag{7}$$

4. Measurement and results

The J/Ψ state in Eq. (3) is a color singlet of spin 1 [8]

$$|J/\Psi(z,m)\rangle = \sum \delta^c_{\bar{c}}\,\frac{\chi_0(x)\vec{\sigma}_{ij}}{\sqrt{x(z-x)}}\,|x\,i\,c\rangle|(z-x)\,j\,c\rangle\,, \tag{8}$$

where z denotes the jets momentum fraction carried by the meson divided between x and $z-x$, while m its spin projection. The ansatz function is taken to be $\chi_0(x) = \frac{1}{\sqrt{C}}\,x^{\beta/2}(z-x)^{\gamma/2}$ with $\gamma = 4m_q^2/\kappa$, $\beta = 4m_{\bar{q}}^2/\kappa$, and C a normalization constant. Parameter values are $P^+ = 10$ GeV, $\alpha_{\mathrm{S}}(P^+) = 0.18$, $m_q = m_{\bar{q}} = 1.27$ GeV, and $\kappa = 1.34$ GeV.

To project onto the J/Ψ wavefunction, we introduce a unitary gate called $\texttt{Prep}_{J/\Psi}$, which implements the meson annihilation operator

$$\left|\widetilde{\Omega}\right\rangle_q\left|\widetilde{\Omega}\right\rangle_{\bar{q}} = \texttt{Prep}_{J/\Psi}(z,m)|J/\Psi(z,m)\rangle\,. \tag{9}$$

Equation (3) is then evaluated by first measuring the probability of obtaining the state $|\widetilde{\Omega}\rangle_q|\widetilde{\Omega}\rangle_{\bar{q}}$ after applying $\texttt{Prep}_{J/\Psi}(z,m)$. The final result is the average of these probabilities over the meson spin states m.

The right panel of Fig. 2 shows the fragmentation function dependence on the evolution (light-cone) time, as well as the convergence with the Trotter step size for $m = 1$. The oscillations are a consequence of the discretization in momentum space and the hard cutoff on the number of particles.

These systematic effects are considered with the following heuristic argument: as time evolves and more particles are produced, the entropy from measurements of $|\psi(t)\rangle$ increase until reaching a saturation plateau [5]. With the limited memory in the present simulation, the plateau is out of reach and the entropy eventually starts to oscillate. The onset of oscillations is then used to pinpoint the regime in which systematic errors become important.

An example of such a regime is shown in the left panel of Fig. 2, where the red (gray) and blue (black) stars indicate two points chosen symmetrically around the time at which the entropy reaches its maximum. The value of the fragmentation function is taken to be the mean between its maximum and minimum within the region. The spread is then used as an estimate of the systematic uncertainty. This procedure is repeated for each momentum

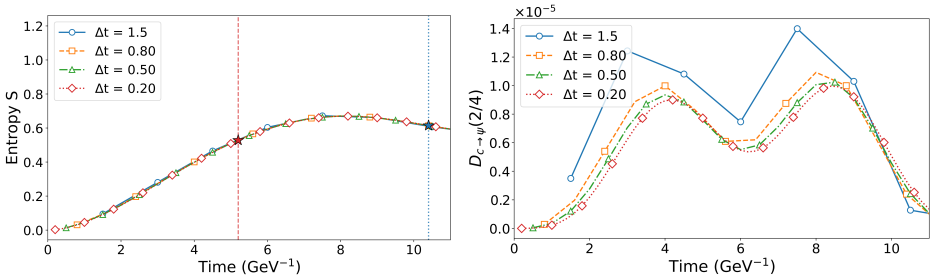

Fig. 2. (Color online) Entropy (left) and fragmentation function (right) for $z = 2/4$ for different Trotter steps Δt as functions of evolution time. The smaller the Trotter steps the more insertions of the evolution kernel to reach the same final time. The red (gray) and blue (black) stars in the entropy plot indicate the points used to estimate the uncertainty in the calculation of the fragmentation function, see the text.

fraction z and several configurations shown in Table 1. The results are summarized in Fig. 3 (left), they are to be compared with the analytical NRQCD computations from [6] (LO, continuous lines) and [7] (NLO, dashed lines) for both quarks with 2 (SU(2)) and 3 (SU(3)) colors.

Table 1. Specific parameters of each simulation. They include either kinetic and vertex interactions (up to g, proportional to 1 and coupling constant g) or all possible terms within the Fock truncation (all).

Run configuration	Terms	N_c	N grid	N_{qubits}	Δt [GeV^{-1}]	ϵ	Runtime [min]
1	up to g	2	4	25	0.2	0	1.5
2	all	2	4	25	0.1	0	22
3	all	2	4	25	0.2	0.02	15
4	up to g	2	8	29	0.2	0	110
5	all	2	8	29	0.2	0.02	1800
6	up to g	3	4	29	0.25	0	120

4.1. Scaling

Figure 3 (right) summarizes the scaling of resources with the number of momentum fractions (m.f.). The two lower curves correspond to the number of interactions in the Hamiltonian, while the two upper curves represent the number of `CNOT` gates. They are almost proportional because each Hamiltonian matrix element requires a basis transformation of the qubit states, a multi-controlled rotation gate, and the inverse basis transformation. These

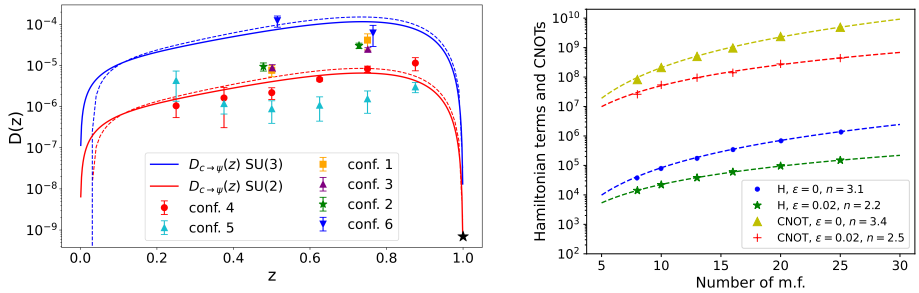

Fig. 3. Left: Fragmentation function of a c quark to a J/ψ meson in terms of momentum fraction z. The reference lines are the NRQCD computation at LO [6] and NLO [7] (dashed). By construction of the numerical grid, the endpoint value $D(1)$ must vanish. See the text and caption of Table 1. Right: Scaling of the number of Hamiltonian terms (two lower lines) and total count of `CNOT` gates (two upper lines) with the number of encoded momentum fractions z (m.f.), see the text.

operations can be decomposed into a constant number of `Toffoli` gates and, using standard decompositions, into `CNOT` gates. The scaling can be smoothed by using an infrared cutoff on matrix elements; the crosses and stars in the plot indicate the number of Hamiltonian terms and `CNOT` gates obtained when only matrix elements satisfying $|V| > \epsilon |V|_{\max}$ are included.

We acknowledge the financial support from grants PID2023-147072NB-I00; PID2022-137003NB-I00 and FPU21/04180 of the Spanish MCIN/AEI/10.13039/501100011033 and Ministry of Universities.

REFERENCES

[1] J. Collins, T.C. Rogers, *Phys. Rev. D* **109**, 016006 (2024).
[2] T.Li, H.Xing, D.B. Zhang, `arXiv:2406.05683 [hep-ph]`.
[3] S.J. Brodsky, H.C. Pauli, S.S. Pinsky, *Phys. Rep.* **301**, 299 (1998).
[4] J.J. Gálvez-Viruet, F.J. Llanes-Estrada, *Phys. Rev. D* **110**, 116018 (2024).
[5] G. Benito-Calviño, J. García-Olivares, F.J. Llanes-Estrada, *Nucl. Phys. A* **1036**, 122670 (2023).
[6] E. Braaten, K.m. Cheung, T.C. Yuan, *Phys. Rev. D* **48**, 4230 (1993).
[7] X.C. Zheng, C.H. Chang, X.G. Wu, *Phys. Rev. D* **100**, 014005 (2019).
[8] M. Li *et al.*, *Eur. Phys. J. C* **82**, 1045 (2022).
[9] J.J. Gálvez-Viruet *et al.*, `arXiv:2510.18869 [hep-ph]`.